Author/s:
Cui, J;Hibbs, B;Gunawan, ST;Braunger, JA;Chen, X;Richardson, JJ;Hanssen, E;Caruso, F

Title:
Immobilized Particle Imaging for Quantification of Nano- and Microparticles

Date:
2016-04-26

Citation:
Cui, J., Hibbs, B., Gunawan, S. T., Braunger, J. A., Chen, X., Richardson, J. J., Hanssen, E. & Caruso, F. (2016). Immobilized Particle Imaging for Quantification of Nano- and Microparticles. Langmuir, 32 (14), pp.3532-3540. https://doi.org/10.1021/acs.langmuir.6b00229.

Persistent Link:
https://hdl.handle.net/11343/108745

Immobilized Particle Imaging for Quantification of Nano- and Microparticles

*Jiwei Cui,[†] Benjamin Hibbs,[†] Sylvia T. Gunawan,[†] Julia A. Braunger,[†] Xi Chen,[†] Joseph J. Richardson,[†,‡] Eric Hanssen,[§] and Frank Caruso[†,]**

[†]ARC Centre of Excellence in Convergent Bio-Nano Science and Technology, and the Department of Chemical and Biomolecular Engineering, the University of Melbourne, Parkville, Victoria 3010, Australia, [‡]CSIRO Manufacturing Flagship, Clayton, Victoria 3168, Australia, [§]Bio21 Molecular Science and Biotechnology Institute, the University of Melbourne, Parkville, Victoria 3010, Australia.

Keywords: optical microscopy, mesoporous silica particles, polymer particles, liposomes, imaging

ABSTRACT

The quantification of nano- and microparticles is critical for diverse applications relying on the exact knowledge of the particle concentration. Although many techniques are available for counting particles, there are some limitations in regards to counting with low-scattering materials and facile counting in harsh organic solvents. Herein, we introduce an easy and rapid particle counting technique, termed “Immobilized Particle Imaging” (IPI), to quantify fluorescent particles with different compositions (i.e., inorganic or organic), structures (i.e., solid, porous, or hollow), and sizes (50-1000 nm) dispersed in either aqueous or organic solutions. IPI is achieved by immobilizing particles of interest in a cell matrix-like scaffold (e.g., agarose), and imaging using standard microscopy techniques. Imaging a defined volume of the immobilized particles allows for the particle concentration to be calculated from the count numbers in a fixed volume. IPI provides a general and facile approach to quantify advanced nano- and microparticles, which will be helpful to researchers to get new insights for different applications (e.g., nanomedicine).

INTRODUCTION

In recent decades, nano- and microparticles with diverse structures and properties have received considerable interest because of their application in the environment, energy, food science, cosmetics, and healthcare.[1-6] Quantification of nano- and microparticles is critical because many of these applications rely on the exact knowledge of the particle concentration. For example, an accurate dosage is important to optimize the efficacy of nanomedicines, while minimizing toxic side-effects of the administered material.[7] Counting techniques for particle suspensions include gravimetric analysis by comparing the total quantity of the particle suspension against the properties of a single particle,[8] molecular quantification by evaluating specific molecules functionalized onto the particles,[9,10] spectroscopic analysis by measuring light absorbance or scattering of the particles (e.g., hemocytometer, UV-Vis, dynamic light scattering, fluorescence correlation spectroscopy, nanoparticle tracking analysis, tunable resistive pulse sensor),[11-13] and high-throughput flow cytometric measurements based on fluorescence and light scattering.[14] Since these methods harness different counting mechanisms based on the inherent properties of the particles being counted, such as the mass or number of moles, or the amount of light scattered or absorbed, some counting limitations arise from the particle shape, size, composition, and solvent used for dispersion (i.e., aqueous or organic).[15] For example, it is challenging to count “soft particles” due to their low density and weak light scattering properties, such as polymer capsules, polymer particles and liposomes. Therefore, it is important to expand on the counting techniques currently available through the introduction of rapid and simple methods that allow counting of nano- and microparticles composed of different materials and in various solvents.

Fluorescence-based counting methods are generally very sensitive because the fluorescence signal can be easily separated from the excitation light and background light. The development of super-resolution fluorescence microscopy has greatly improved the imaging of fluorescent nanoparticles.[16-18] However, imaging of nano- and microparticles in dispersions can be hampered by the Brownian motion of the particles. Recently, an elegant method to quantify nanoparticle uptake and/or association on a single cell level has been reported, aiming at preserving the spatial information of the administered nanoparticles by analyzing image stacks acquired by confocal laser scanning microscopy (CLSM) or stimulated emission depletion microscopy (STED) using a home-built digital image analysis system.[19,20] Inspired by this immobilization strategy of nanoparticles within a cell matrix, we herein introduce a facile particle counting technique, termed “Immobilized Particle Imaging” (IPI), to quantify particles with different compositions, structures, and sizes (50–1000 nm) dispersed in either aqueous or organic solvents (**Scheme 1**). IPI is based on standard fluorescence microscopy techniques and is achieved by immobilizing the particles of interest in a cell matrix-like scaffold. Agarose is used as a matrix for aqueous dispersions, while an organic-based curable material (i.e., super glue) is employed as a matrix for particles dispersed in organic solvents, such as toluene. Subsequently, a defined volume of the immobilized particles is imaged, allowing the particle concentration to be calculated from the count numbers in a fixed volume. Immobilization is necessary to prevent the inherent movement of particles in solution.

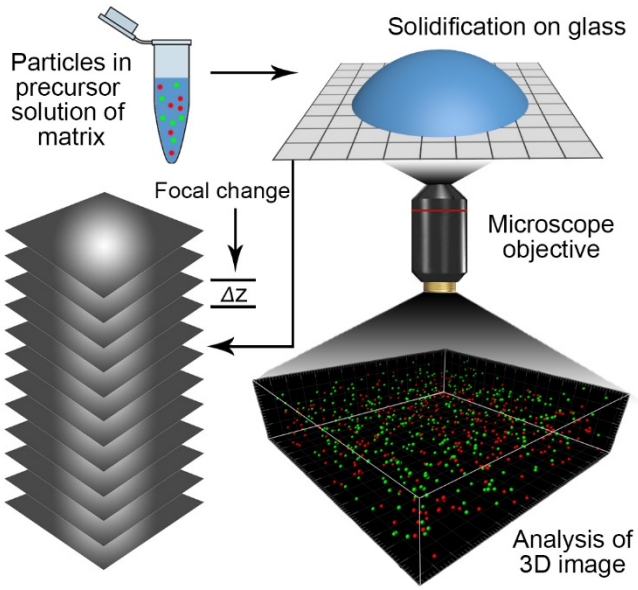

Scheme 1. Schematic illustration of IPI for the quantification of particles dispersed in aqueous or organic solution.

IPI is compared against high-sensitivity flow cytometry (Apogee A50 Micro) for larger particles (100–1000 nm) and theoretical calculations based on silica weight and density for PEGylated silica particles (~50 nm). In addition to conventional fluorescence microscopy, which is limited to approximately 250 nm in X/Y resolution and 500 nm in Z, Structured Illumination Microscopy (SIM), a super-resolution technique that improves the resolution limit down to 110 nm in X/Y and 250 nm in Z,[21] can be used to yield higher resolution 3D images for counting small particles immobilized in a matrix or associated with cells.

EXPERIMENTAL SECTION

Materials. Tetraethyl orthosilicate (TEOS), (3-aminopropyl)triethoxysilane (APTES), cetyltrimethylammonium bromide (CTAB), cetyltrimethylammonium tosylate (CTAT), *N*-(3-dimethylaminopropyl)-*N*′-ethylcarbodiimide hydrochloride (EDC), *N*-Chloro-*p*-

toluenesulfonamide sodium salt (Chloramine T), dithiothreitol (DTT), poly(*N*-vinylpyrrolidone) (PVP, 10 kDa), 2-(*N*-morpholino)ethanesulfonic acid hydrate (MES), 3-(*N*-morpholino)propanesulfonic acid (MOPS), Dulbecco's phosphate-buffered saline (DPBS), Triton X-100, bovine serum albumin (BSA), sodium phosphate dibasic, triethanolamine, hydrofluoric acid (HF, 48 wt%), ammonium fluoride (NH_4F), and ammonium hydroxide solution (28-30%) were obtained from Sigma-Aldrich (Australia). Poly(methacrylic acid, sodium salt) (PMA, M_w 15 kDa, 30 wt% solution in water) was from Polysciences, Inc. (USA). Pyridine dithioethylamine (PDA) was purchased from Shanghai SpeedChemical Co. Ltd. (China). Non-porous silica particles (~520 nm) were obtained from MicroParticles GmbH (Germany). Alexa Fluor 488 Cadaverine (AF488-Cad), Alexa Fluor 488 Maleimide (AF488-MAL), Alexa Fluor 488 NHS Ester (AF488-NHS), Alexa Fluor 647 Cadaverine (AF647-Cad), Alexa Fluor 488 Phalloidin, Hoechst, 2-(4,4-Difluoro-5-methyl-4-bora-3a,4a-diaza-*s*-indacene-3-dodecanoyl)-1-hexadecanoyl-*sn*-glycero-3-phosphocholine (BODIPY-C_{12}HPC), fetal bovine serum (FBS), and Dulbecco's Modified Eagle Medium (DMEM) with GlutaMAX™ Supplement were provided by Life Technologies (Australia). 1,2-dioleoyl-*sn*-glycero-3-phosphocholine (DOPC) was purchased from Avanti Polar Lipids (USA). mPEG-SCM (2 kDa) was obtained from Creative PEGWorks (USA). Low-melting point agarose was purchased from BIO-RAD (Australia). Super glue was obtained from Selleys® (Australia). The water used in all experiments was prepared in a three-stage Millipore Milli-Q Plus 185 purification system and had a resistivity greater than 18.2 MΩ cm.

Synthesis of PMA_{PDA}. PMA_{PDA} was synthesized via EDC-mediated amide bond formation between the carboxyl groups of PMA and the amine groups of PDA.[22] In a typical experiment, a PMA solution (360 mg of 30 wt% solution, 1 equiv. of MA) was diluted into 5 mL of phosphate

buffer (0.1 M, pH 7.2). The resulting solution was incubated with EDC (57.5 mg, 0.3 equiv.) with stirring for 15 min. Subsequently, PDA (33.4 mg, 0.15 equiv.) was added to the mixture and the pH was adjusted to 7.2. The reaction was allowed to proceed overnight. The resulting mixture was placed inside a dialysis membrane (molecular weight cut-off 3500, Thermo) and dialyzed extensively against water, filtered with a 0.2 μm syringe filter, and isolated via lyophilization. The degree of thiol functionalization was characterized by measuring the absorbance of the released pyridine-2-thione (λ_{max} = 343 nm), and then quantified from a calibration curve of PDA, which corresponded to 10 mol% modification.

Fabrication of LbL PMA_{SH} Capsules (PMAC-1000). Non-porous silica particles (519 nm, 100 μL, 5% w/v) were washed with three standard centrifugation/redispersion cycles (550 *g*, 1 min) with acetate buffer (50 mM, pH 4). LbL capsules were prepared by the alternate deposition of PMA_{SH}, (1 mg mL^{-1} in acetate buffer) and PVP (1 mg mL^{-1} in acetate buffer) on silica particle templates. The polymers were allowed to interact for 10 min with constant shaking. The excess polymers were then removed via three standard centrifugation/redispersion cycles. LbL assembly was repeated until five bilayers of PMA_{SH}/PVP were achieved. PVP was then added as the final coating to prevent interparticle cross-linking. These multilayers were cross-linked with chloramine T (2.5 mM in 50 mM MES buffer, pH 6) for 1 min and subsequently washed via three standard centrifugation/redispersion cycles. The remaining thiol functional groups in PMA_{SH} were used for fluorescent labeling with AF488-MAL. The cross-linked multilayers were left to incubate with AF488-MAL (5 μL in 50 mM phosphate buffer, pH 7.4) overnight. Afterwards, the excess dye was washed off via three standard centrifugation/redispersion cycles. Silica templates were then removed with a 2 M HF/8 M NH_4F solution (pH ~5). Sacrificial PVP layers were then expelled via three centrifugation/redispersion cycles (4500 *g*, 6 min) in

phosphate buffer (50 mM, pH 7.4), resulting in LbL PMA_{SH} capsules. *Caution! HF is highly toxic. Extreme care should be taken when handling HF solution and only small quantities should be prepared*.

Fabrication of PMA_{SH} Replica Capsules (PMAC-200) or Particles (PMAP-100). The SC/MS or MS templates were functionalized with primary amine groups by APTES modification before the preparation of PMA_{SH} replicas. In this process, the MS particles were dispersed in ethanol with a concentration of 30 mg mL^{-1} by sonication before ammonia and APTES were added to the suspension. The volume ratio of ethanol:ammonia:APTES was fixed at 20:1:1, and the suspension was allowed to stir overnight. PMA_{SH} capsules or particles were prepared via thiol-disulfide exchange cross-linking according to our previously published method.[23] Briefly, 3 mg of SC/MS or MS templates were incubated with 0.9 mg of PMA_{PDA} (5 mg mL^{-1} in 100 mM acetate buffer, pH 5) under constant shaking for 6 h. Subsequently, the polymer-loaded templates were isolated by centrifugation and washed three times with acetate buffer. The pellet was dispersed in 300 µL of PMA_{SH} solution (0.5 mg mL^{-1} in acetate buffer). Here, PMA_{SH} was freshly prepared by the incubation with 0.5 M DTT in MOPS buffer (20 mM, pH 8) for 15 min and purified with a NAP-5 Sephadex column. In this step, PMA_{PDA} was cross-linked by PMA_{SH} based on thiol-disulfide exchange at pH 5 in acetate buffer (Figure S1). The PMA_{SH}-loaded particles were labeled with AF488-Cad or AF647-Cad based on EDC chemistry. After three washing cycles with water, the templates were dissolved with a 2 M HF/8 M NH_4F solution (pH ~5). *Caution! HF is highly toxic. Extreme care should be taken when handling HF solution and only small quantities should be prepared*. The resultant PMA replicas were centrifuged and washed three times with water.

Liposome Preparation. DOPC lipid films were prepared by evaporation of chloroform (2 mg of lipid dissolved in chloroform). To fluorescently label the liposomes, 0.1 mol% of BODIPY-C_{12}HPC was added to the DOPC solution before solvent evaporation. Liposomes were prepared by rehydrating the lipid film in 1 mL of buffer (10 mM MOPS with 1 mM EDTA, pH 7.3) for 20 min, followed by extrusion through a 200 nm polycarbonate membrane (31 cycles).

Preparation of PEGylated Silica Particles. Silica particles with an average size of 50 nm (SNOWTEX, Japan) were modified with APTES as described above and labeled with AF488-NHS in ethanol. The obtained particles were dispersed in toluene and PEGylated with mPEG-SCM, followed by three washing steps with toluene. The following equation was used to calculate the concentration of PEGylated silica particles:

$$N = \frac{m}{\rho(\frac{4}{3}\pi r^3)} \qquad (1)$$

where m is the particle mass in 100 µL of toluene, ρ is the silica density (2.65 g cm^{-3}), and r is the particle radius (25 nm).

Particle Quantification Using IPI. Agarose solution was prepared by dissolving 5% (w/v) low-melting point agarose in water at a temperature of 60 °C. To image the particles in a certain volume, particles (e.g., PMA capsules, PMA particles) were mixed with the 5% agarose solution with a volume ratio of 1:1 (liposomes were mixed at 40 °C), leaving 2.5% (w/v) agarose as the final concentration of agarose in solution. To remove bubbles, the agarose solution was centrifuged with 10g for 10 s. The mixture was placed as a droplet (~20 µL) onto a glass coverslip and allowed to cool on ice and become a gel before imaging. A PEGylated silica particle suspension was diluted with toluene and mixed with super glue at a volume ratio of 1:5.

The mixture was spread onto a glass coverslip and the toluene was allowed to evaporate overnight before imaging. Fluorescence images were taken in a volume of 80 × 80 × 20 μm^3 (40 × 40 × 10 μm^3 for SIM images) with a DeltaVision OMX SIM microscope (Applied Precision) operating in deconvolution mode, using a spatially calibrated 60× objective (Olympus, 1.42NA). Two images were obtained from each of three replicates. Therefore, six images for each sample were processed with Imaris 7.0.0 (Bitplane AG) to count the particles. For visualization, microscopy images with a volume of 40 × 40 × 20 μm^3 were presented. The concentration of the capsules/particles *c* can then be calculated based on the number *N* counted in the imaged volume *V* of agarose matrix:

$$c_{\mathrm{P}} = a \times \frac{N_{\mathrm{P}}}{V_{\mathrm{I}}} \qquad (2)$$

where *a* is the dilution factor to account for any dilutions made during sample preparation.

Cell Imaging. HeLa cells were seeded at 3 × 10^4 cells/well into 8-well Lab-Tek I chambered glass coverslips (Thermo Fisher Scientific, Rochester) and allowed to adhere overnight. Cells were then incubated with PMA capsules or particles for 24 h followed by three washing steps with DPBS. Cells in each well were fixed with 200 μL of 4% paraformaldehyde for 10 min at 25 °C, then washed by DPBS, and incubated with 400 μL of permeabilization buffer (0.1% Triton X-100 and 1% BSA) for 5 min, followed by washing with DPBS. Cells were stained with Alexa Fluor 488 Phalloidin (5 μL of stock solution in 200 μL of PBS containing 1% BSA, 20 min incubation) for actin, and with Hoechst (5 μg mL^{-1} in DPBS, 10 min incubation) for nuclei. Cells were washed three times after each staining. To minimize photobleaching, DPBS in each well was removed and 100 μL of Vectashield (Vector Labs) was added. Super-resolution images were acquired via a DeltaVision OMX SIM microscope (Applied Precision) operating in

Structured Illumination Microscopy mode, to obtain an approximate resolution of 110 nm in X/Y and 250 nm in Z.

Characterization Method. TEM (FEI Tecnai G2 Spirit, operated at 120 kV) was used to examine the particle morphologies. The TEM samples (1 μL) in water were placed onto strong carbon film-coated copper grids (ProSciTech, Australia) and allowed to air-dry. For cryo-TEM measurements, the samples were plunge frozen in liquid ethane on holey carbon coated copper grids. The samples were then observed under low dose (total dose <1500 e-/nm^2) on a FEI Tecnai F30 operated at 300 kV. Digital micrographs were recorded on a Gatan UltraScan 1000 2k × 2k CCD camera. The size distributions of the particles in water were examined using a Malvern Zetasizer Nano ZS.

RESULTS AND DISCUSSION

To verify the feasibility of IPI, five types of particles with different compositions, structures, and sizes were prepared for analysis and quantification. Poly(methacrylic acid) (PMA) capsules with an average diameter of ~1000 nm (PMAC-1000) were prepared via layer-by-layer assembly using non-porous silica particles (~520 nm) as templates (Figure 1a1) and thiolated PMA as a building block (Figure S1a), as reported previously.[24] Figure S2 shows the uniform size distribution and well-defined hollow structure of PMAC-1000 in aqueous solution. Due to the evaporation of water after air-drying, PMAC-1000 exhibit the typical creases and folds of hollow polymer capsules (Figure 1a2).[25,26] Smaller polymer capsules and particles (100 and 200 nm) were prepared via a mesoporous silica (MS) templating method, which was developed to allow fine control over characteristics and properties of polymer replica capsules/particles, including size, composition, shape, and elasticity, as well as cargo loading and release.[22,23,27-29] Solid

core/mesoporous shell silica (SC/MS) particles (~250 nm) with a shell thickness of ~38 nm and mesoporous silica particles (~110 nm) were prepared according to previously reported methods and were used as templates (Figure 1b1,c1).[30-32] The thiol–disulfide exchange strategy (Figure S1b) combined with the MS templating method allowed for the preparation of PMA capsules with an average size of 200 nm (PMAC-200) (Figures 1b2 and 2) and PMA particles with an average size of 100 nm (PMAP-100) (Figures 1c2 and S3). All of the polymer capsules/particles were labeled with Alexa Fluor 488 (AF488) and were well dispersed in aqueous solutions. In addition to the polymer capsules/particles, inorganic silica particles (~50 nm) were aminated with (3-aminopropyl)triethoxysilane, labeled with AF488, functionalized with PEG, and dispersed in toluene (Figure 1d). Finally, liposomes (~170 nm) composed of 1,2-dioleoyl-*sn*-glycero-3-phosphocholine (DOPC) were prepared by lipid hydration and extrusion (Figure 1e).[33,34] The size distribution of the liposomes is shown in Figure S4.

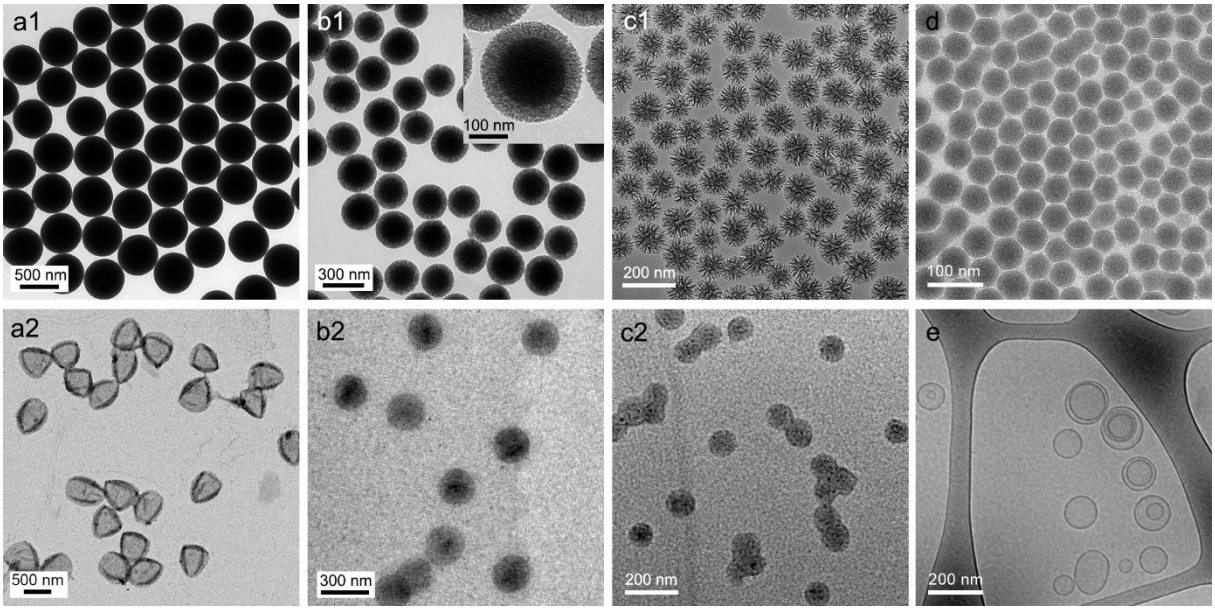

Figure 1. Transmission electron microscopy (TEM) images of (a1) silica particles (~520 nm), (a2) PMAC-1000, (b1) SC/MS particles (~250 nm), (b2) PMAC-200, (c1) MS particles (~110

nm), (c2) PMAP-100, and (d) PEGylated silica particles (~50 nm). (e) Cryo-TEM image of DOPC liposomes (~170 nm).

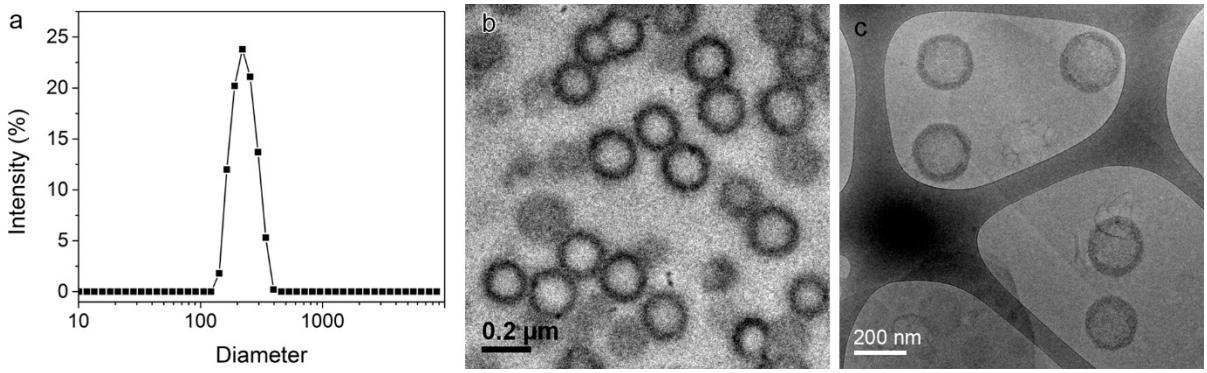

Figure 2. (a) Size distribution, (b) ultramicrotomed TEM and (c) cryo-TEM image of PMAC-200 dispersed in water.

To confirm the bioinspired immobilization strategy that IPI is based on, HeLa cells were incubated with PMAC-200 or PMAP-100 labeled with AF647 for 24 h, followed by fixation and staining of the actin cytoskeleton. Using SIM, detailed 3D images of cells were obtained with approximately 110 nm resolution in X and Y (Figure 3a and 3c). The hollow structure of PMAC-200 can be clearly observed in the super-resolution microscopy images (Figure 3a), unlike the traditional fluorescence microscopy images (Figure S3b), and after image analysis, the capsule/particle count can be elucidated for a single cell (Figure 3b and 3d). This shows that using IPI in combination with super-resolution microscopy allows for more accurate counts for particle sizes below the resolution limit of optical microscopy.

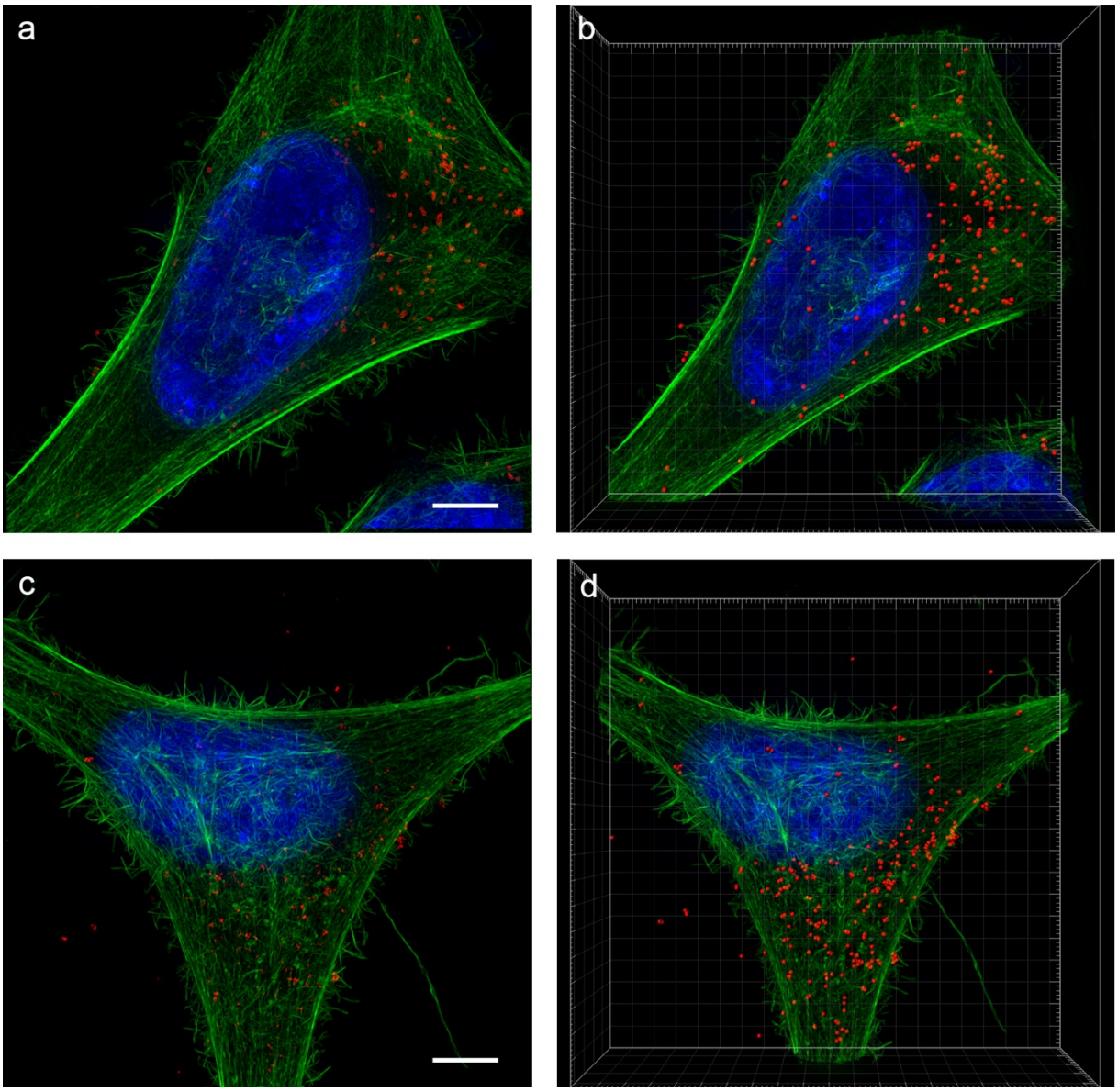

Figure 3. SIM images with maximum intensity projection of HeLa cells after 24 h incubation with (a) PMAC-200 and (c) PMAP-100. 3D reconstructions of (b) PMAC-200 and (d) PMAP-100 distributions in a single cell (top view). Data analysis using Imaris indicates that the particle numbers associated with HeLa cells are 180 (PMA-200) and 260 (PMA-100), respectively. All scale bars are 5 μm.

Low-melting point agarose, which can be used to coat particles and generate capsules, and to protect underlying protein layers,[35-37] was employed as a scaffold for immobilizing the polymer capsules/particles to prevent the movement caused by Brownian motion, which is inherent to imaging in solutions. Prior to imaging, the PMA capsules/particles were mixed with low-melting point agarose in the liquid state at ~60 °C. After allowing the agarose to cool and harden on glass coverslips, defined volumes of the samples were imaged using deconvolution microscopy. The imaged volume can be simply calculated by using a defined z-height (e.g., 20 μm) and fixing the image size (e.g., 80 × 80 μm^2) on a spatially calibrated microscope. The immobilization of capsules/particles ensures that the capsules/particles are imaged accurately, without repetition due to Brownian motion. It should be noted that particle imaging can be performed on a confocal microscope equipped with a piezoelectric motor. The image is then processed using imaging analysis software, such as Imaris 7.0.0 (Bitplane AG), by defining a threshold level of intensity of the capsules/particles, after which counting can be automatically performed using built-in functions as detailed in the Experimental Section (Equation 2).

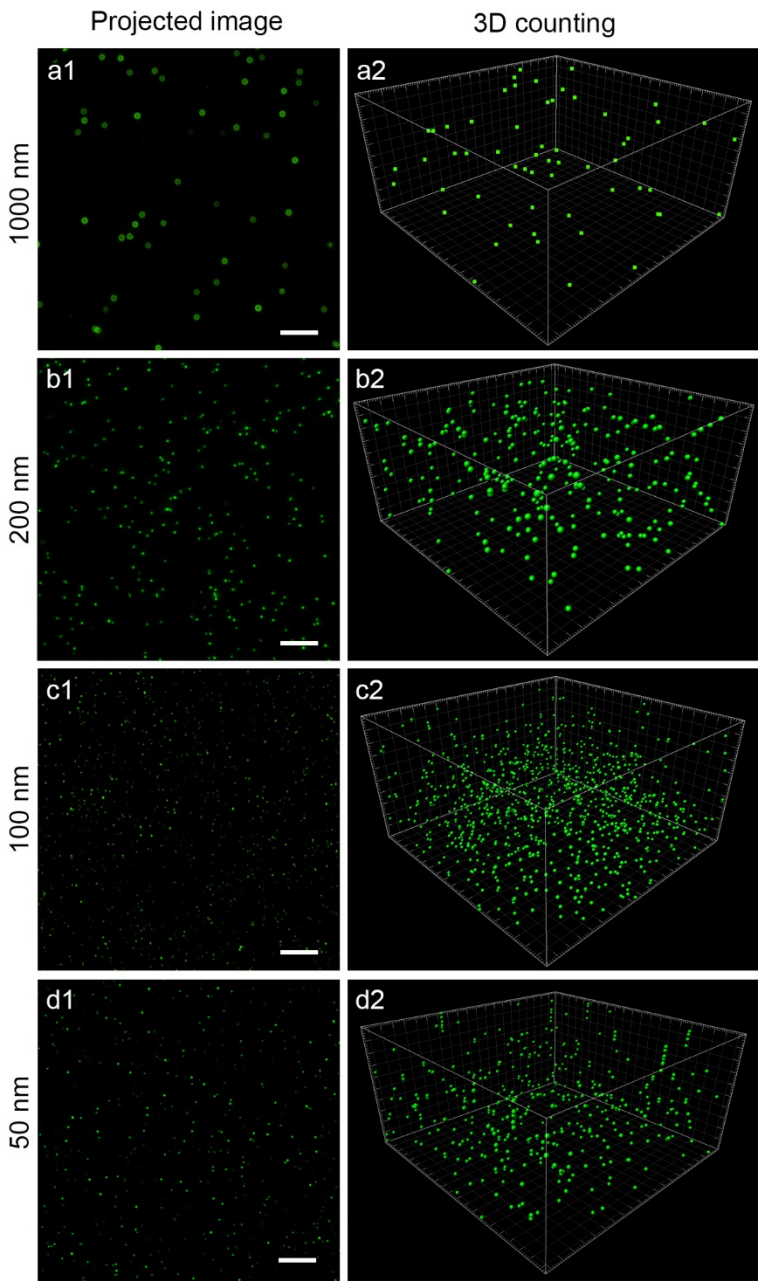

Figure 4. Deconvolution microscopy images with maximum intensity projection of (a1) PMAC-1000, (b1) PMAC-200, (c1) PMAP-100, and (d1) PEGylated silica particles. Scale bars are 5 μm. (a2-d2) 3D reconstructions of capsule/particle distributions (40 × 40 × 20 μm^3) in agarose (a2-c2) and in super glue (d2).

Depending on the structure of capsules or particles, different functions were applied to analyze the acquired images. For particles with solid or matrix structure the spot detection tool in Imaris could be used directly, while for capsules the surface area of the capsules based on fluorescence intensity was reconstructed (Figure S5). Figure 4a2 shows the central dots of PMAC-1000, as determined after surface reconstruction. Although the PMAC-200 have a hollow structure (Figure 2b,c), the resolution of the deconvolution microscope is insufficient to show their hollow structure in agarose (Figure 4b1). Therefore, definition of fluorescence spots by either size or surface area based on the threshold of fluorescence intensity in Imaris is identical for counting the PMAC-200 in agarose. Spots in Figure 4b2 represent the distribution of PMAC-200 immobilized in agarose. Similarly, PMAP-100 can be imaged in agarose and counted using the Imaris software (Figure 4c). Since the particles were immobilized in agarose during fast gelation on ice, we did not observe particle accumulation either at the bottom or on the surface of the agarose droplet and there was no issue with settling. Aggregates could also be distinguished based on the value of fluorescence intensity and the size/surface area of the identified object (Figure S6). This has also been shown for other nanoparticle systems and confirmed using STED, allowing accurate determination of the number of nanoparticles that are smaller in size than the optical resolution.[19] This greatly increases the sensitivity of imaging techniques for counting particles, including IPI. Besides counting the particles, the degree of aggregation could also be determined from the images, allowing evaluation of the quality of dispersion.

Except for Imaris software, counting particles in z-stacks can also be easily performed using the 3D Objects Counter plugin in ImageJ/FIJI. Similar to Imaris, a size filter and an intensity-based threshold can be applied to exclude background noise and different representation options, including maps of surface voxels. Figure 5 shows the projection image of PMAC-200 distributed

in agarose analyzed by FIJI software. The particle number obtained from FIJI matches well with that from Imaris. For concentrated particle dispersions, it is better to dilute the suspension to obtain about 100–2000 particles/capsules per imaged volume (80 × 80 × 20 μm^3) to allow for precise counts and consequently accurate concentrations.

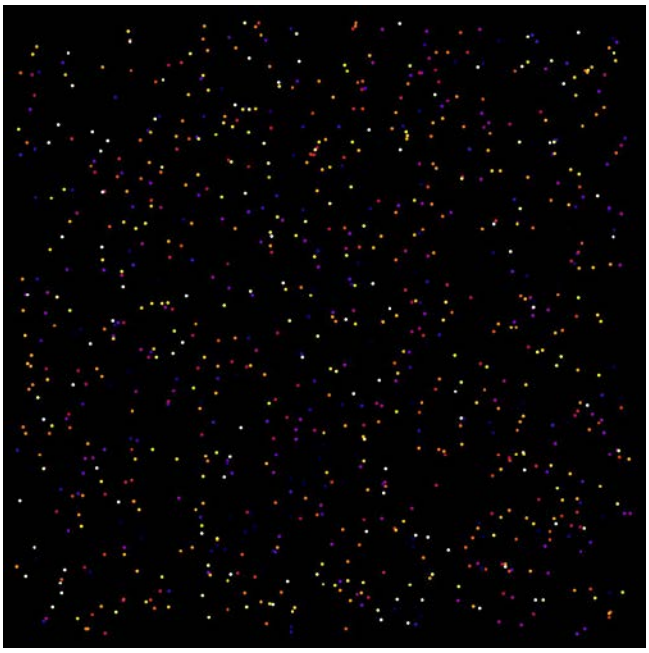

Figure 5. Projection image of PMAC-200 distributed in agarose analyzed by FIJI software. Each dot represents one particle. Different colors indicate the particles distributed at different focal planes. For example, blue and white dots represent the particles at the bottom and on the top of the imaged volume (40 × 40 × 20 μm^3), respectively.

IPI for counting polymer capsule/particles with three different sizes was compared against flow cytometry, and it was found that IPI gives values within 15% of those determined using an Apogee flow cytometer (Figure S7 and Table S1). Notably, all values derived from IPI measurements are slightly higher compared to those obtained by flow cytometry. We suggest that this is due to small aggregates that are counted as single events by the flow cytometer

whereas using IPI followed by image analysis allows such objects to be more accurately resolved.

Interestingly, the PMAC-1000 maintained their size and hollow structure after immobilization in agarose **(**Figure 4a1 and S2b) as opposed to the creases and folds that are usually observed upon drying (Figure 1a2). Moreover, IPI was also applied to count fluorescently labeled liposomes immobilized in an agarose matrix to demonstrate that even systems that are usually prone to irreversible deconstruction after drying could be immobilized and quantified (Figure S8). This shows that IPI with agarose as the immobilization medium is well suited to quantify particle/capsules whose structural integrity relies on hydration. In fact, the transition temperature of the low-melting point agarose is ~26 °C. We can mix particles with agarose above this temperature for imaging as long as the particles are heat stable.

In addition to counting capsules/particles from aqueous solution, particles dispersed in organic solvent can be counted using IPI, by using an organic-based curable material for immobilization instead of a hydrogel. Herein, PEGylated silica particles dispersed in toluene were mixed with super glue (Selleys®, Australia), the mixture was spread onto a glass coverslip and the toluene was allowed to evaporate and dry before imaging. Figure 4d1 shows that silica particles can be well dispersed in super glue. The theoretical concentration based on silica weight and density is approximate by 1.5 times higher than the experimental result (Table S1), which may be attributed to the contributions from amine- and PEG-modification that increase the particle weight.

It is typically difficult to count nano- and microparticles of different sizes and types in the same solution using standard imaging/counting techniques. IPI, however, can be used to count

AF488-labeled PMAC-1000 and PMAC-200 particles that are only different in size. The particle concentration in solution can be correlated based on the count numbers in a fixed volume. After immobilization in agarose, the two classes of particles were imaged in stacks and Imaris was used to define the two different sizes in the sample. The fluorescence image (Figure 6a1) shows the mixture of PMAC-1000 and PMAC-200 immobilized in agarose. After analyzing the samples by defining the capsule signal threshold, the capsules could be counted and concentrations for both capsules determined, with the central dots of PMAC-1000 (red) and PMAC-200 (green) shown in Figure 6a2. Similarly, IPI was used to count the capsules in a mixture of PMAC-200 either labeled with AF488 or Alexa Fluor 647 (AF647) (Figure 6b1 and 6b2) to show that similarly sized materials with different properties could also be distinguished and counted. The concentrations determined by IPI fit closely with the individual concentrations separately determined by flow cytometry prior to mixing (Table S1). The counting of mixed capsule/particle suspensions highlights the potential for improving the analysis of these systems in other immobilizing agents, such as the intracellular matrix found in cells.

CONCLUSIONS

We have introduced a technique for the quantification of particles with different compositions, structures, and sizes ranging from 50 to 1000 nm using a standard microscopy technique combined with the immobilization of nano- and micro-materials in a matrix and subsequent image analysis. Importantly, different classes of fragile and robust nano- and microparticles were prepared, including polymer capsules, polymer particles, liposomes, and inorganic silica particles, which were used to validate IPI. The counting results obtained from IPI match closely with data generated by flow cytometry for particles above 100 nm. Super-resolution microscopy was used, not only for counting particles associated with cells, but also for distinguishing the

nanostructures of polymer capsules and particles. IPI provides an avenue to quantify capsules and particles and is expected to contribute to new insights in the investigation of bio-nano interactions.

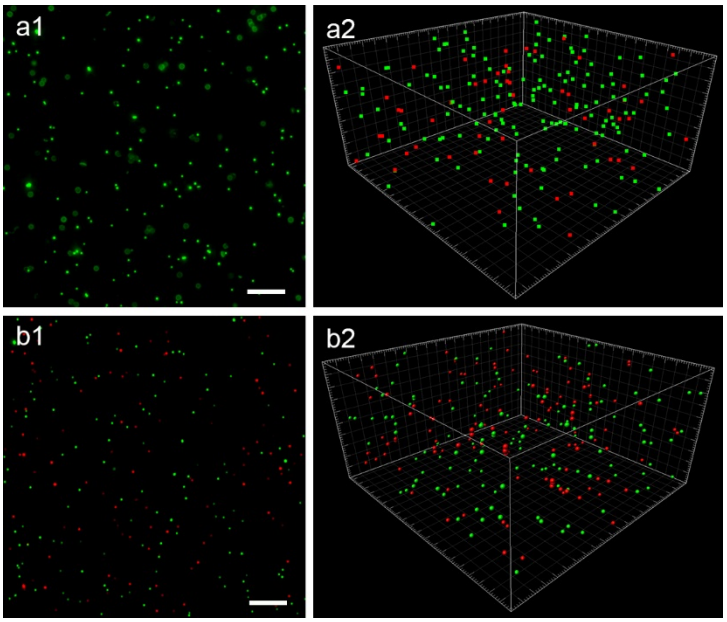

Figure 6. Distinguishing capabilities of IPI. Deconvolution microscopy images with maximum intensity projection of a mixture of (a1) both AF-488 labeled PMAC-1000 and PMAC-200 (green), and (b1) AF488 and AF647 (red) labeled PMAC-200. (a2,b2) 3D reconstructions of capsules/particles in agarose (40 × 40 × 20 μm^3) representing their distributions in (a1,b1), respectively. Red and green dots in (a2) represent PMAC-1000 and PMAC-200, respectively, whereas they represent AF647 and AF488 labeled PMAC-200, respectively, in (b2). All scale bars are 5 µm.

ASSOCIATED CONTENT

Supporting Information

Additional experimental data containing polymer molecular structures and cross-linking strategy

for the preparation of capsules and particles, DLS, cryo-TEM, and fluorescence microscopy characterization of PMAP-100 and DOPC liposomes, 3D reconstruction image showing the distribution of PMAC-1000 distribution immobilized in agarose, flow cytometry for capsule/particle counting showing the fluorescence peaks, 3D reconstructions of PMAC-200 or liposome distributions in agarose, comparison of particle counting based on IPI and flow cytometry methods. This material is available free of charge via the Internet at http://pubs.acs.org.

AUTHOR INFORMATION

Corresponding Author

*Email: fcaruso@unimelb.edu.au (F.C.).

Notes

The authors declare no competing financial interest.

ACKNOWLEDGMENT

This work was supported by the Australian Research Council (ARC) Centre of Excellence in Convergent Bio-Nano Science and Technology (project number CE140100036) and the ARC under the Australian Laureate Fellowship (F.C., FL120100030). This work was performed in part at the Materials Characterization and Fabrication Platform (MCFP) at the University of Melbourne and the Victorian Node of the Australian National Fabrication Facility (ANFF).

REFERENCES

(1) Ariga, K.; Ishihara, S.; Abe, H.; Li, M.; Hill, J. P. Materials Nanoarchitectonics for Environmental Remediation and Sensing. J. Mater. Chem. ***2012***, 22, *2369-2377.*

(2) Daniel, M.-C.; Astruc, D. Gold Nanoparticles: Assembly, Supramolecular Chemistry, Quantum-Size-Related Properties, and Applications toward Biology, Catalysis, and Nanotechnology. *Chem. Rev.* **2004**, *104*, 293-346.

(3) de Aberasturi, D. J.; Serrano-Montes, A. B.; Liz-Marzán, L. M. Modern Applications of Plasmonic Nanoparticles: From Energy to Health. *Adv. Opt. Mater.* **2015**, *3*, 602-617.

(4) Lohse, S. E.; Murphy, C. J. Applications of Colloidal Inorganic Nanoparticles: From Medicine to Energy. *J. Am. Chem. Soc.* **2012**, *134*, 15607-15620.

(5) Irvine, D. J.; Hanson, M. C.; Rakhra, K.; Tokatlian, T. Synthetic Nanoparticles for Vaccines and Immunotherapy. *Chem. Rev.* **2015**, *115*, 11109-11146.

(6) Mitragotri, S.; Anderson, D. G.; Chen, X.; Chow, E. K.; Ho, D.; Kabanov, A. V.; Karp, J. M.; Kataoka, K.; Mirkin, C. A.; Petrosko, S. H. *et al.* Accelerating the Translation of Nanomaterials in Biomedicine. *ACS Nano* **2015**, *9*, 6644-6654.

(7) Liu, R.; Liu, H. H.; Ji, Z.; Chang, C. H.; Xia, T.; Nel, A. E.; Cohen, Y. Evaluation of Toxicity Ranking for Metal Oxide Nanoparticles Via an in Vitro Dosimetry Model. *ACS Nano* **2015**, *9*, 9303-9313.

(8) Liu, X.; Atwater, M.; Wang, J.; Huo, Q. Extinction Coefficient of Gold Nanoparticles with Different Sizes and Different Capping Ligands. *Colloids Surf., B* **2007**, *58*, 3-7.

(9) Uddayasankar, U.; Shergill, R. T.; Krull, U. J. Evaluation of Nanoparticle–Ligand Distributions to Determine Nanoparticle Concentration. *Anal. Chem.* **2015**, *87*, 1297-1305.

(10) Paunescu, D.; Mora, C. A.; Querci, L.; Heckel, R.; Puddu, M.; Hattendorf, B.; Günther, D.; Grass, R. N. Detecting and Number Counting of Single Engineered Nanoparticles by Digital Particle Polymerase Chain Reaction. *ACS Nano* **2015**, *9*, 9564-9572.

(11) Haiss, W.; Thanh, N. T.; Aveyard, J.; Fernig, D. G. Determination of Size and Concentration of Gold Nanoparticles from Uv-Vis Spectra. *Anal. Chem.* **2007**, *79*, 4215-4221.

(12) Berland, K.; So, P.; Chen, Y.; Mantulin, W.; Gratton, E. Scanning Two-Photon Fluctuation Correlation Spectroscopy: Particle Counting Measurements for Detection of Molecular Aggregation. *Biophys. J.* **1996**, *71*, 410-420.

(13) Ma, K.; Mendoza, C.; Hanson, M.; Werner-Zwanziger, U.; Zwanziger, J.; Wiesner, U. Control of Ultrasmall Sub-10 Nm Ligand-Functionalized Fluorescent Core–Shell Silica Nanoparticle Growth in Water. *Chem. Mater.* **2015**, *27*, 4119-4133.

(14) Givan, A. L., *Flow Cytometry: First Principles*. Wiley-Liss: New York, 2001.

(15) Shang, J.; Gao, X. Nanoparticle Counting: Towards Accurate Determination of the Molar Concentration. *Chem. Soc. Rev.* **2014**, *43*, 7267-7278.

(16) Moerner, W. E. Single-Molecule Spectroscopy, Imaging, and Photocontrol: Foundations for Super-Resolution Microscopy (Nobel Lecture). *Angew. Chem. Int. Ed.* **2015**, *54*, 8067-8093.

(17) Hell, S. W. Nanoscopy with Focused Light (Nobel Lecture). *Angew. Chem. Int. Ed.* **2015**, *54*, 8054-8066.

(18) Betzig, E. Single Molecules, Cells, and Super-Resolution Optics (Nobel Lecture). *Angew. Chem. Int. Ed.* **2015**, *54*, 8034-8053.

(19) Torrano, A. A.; Blechinger, J.; Osseforth, C.; Argyo, C.; Reller, A.; Bein, T.; Michaelis, J.; Bräuchle, C. A Fast Analysis Method to Quantify Nanoparticle Uptake on a Single Cell Level. *Nanomedicine* **2013**, *8*, 1815-1828.

(20) Torrano, A. A.; Bräuchle, C. Precise Quantification of Silica and Ceria Nanoparticle Uptake Revealed by 3d Fluorescence Microscopy. *Beilstein J. Nanotechnol.* **2014**, *5*, 1616-1624.

(21) Schermelleh, L.; Carlton, P. M.; Haase, S.; Shao, L.; Winoto, L.; Kner, P.; Burke, B.; Cardoso, M. C.; Agard, D. A.; Gustafsson, M. G. L. *et al.* Subdiffraction Multicolor Imaging of the Nuclear Periphery with 3d Structured Illumination Microscopy. *Science* **2008**, *320*, 1332-1336.

(22) Cui, J.; De Rose, R.; Alt, K.; Alcantara, S.; Paterson, B. M.; Liang, K.; Hu, M.; Richardson, J. J.; Yan, Y.; Jeffery, C. M. *et al.* Engineering Poly(Ethylene Glycol) Particles for Improved Biodistribution. *ACS Nano* **2015**, *9*, 1571-1580.

(23) Cui, J.; De Rose, R.; Best, J. P.; Johnston, A. P.; Alcantara, S.; Liang, K.; Such, G. K.; Kent, S. J.; Caruso, F. Mechanically Tunable, Self-Adjuvanting Nanoengineered Polypeptide Particles. *Adv. Mater.* **2013**, *25*, 3468-3472.

(24) Best, J. P.; Neubauer, M. P.; Javed, S.; Dam, H. H.; Fery, A.; Caruso, F. Mechanics of Ph-Responsive Hydrogel Capsules. *Langmuir* **2013**, *29*, 9814-9823.

(25) Cui, J.; Liu, Y.; Hao, J. Multiwalled Carbon-Nanotube-Embedded Microcapsules and Their Electrochemical Behavior. *J. Phys. Chem. C* **2009**, *113*, 3967-3972.

(26) Shao, J.; Xuan, M.; Dai, L.; Si, T.; Li, J.; He, Q. Near-Infrared-Activated Nanocalorifiers in Microcapsules: Vapor Bubble Generation for in Vivo Enhanced Cancer Therapy. *Angew. Chem. Int. Ed.* **2015**, *54*, 12782-12787.

(27) Cui, J.; Björnmalm, M.; Liang, K.; Xu, C.; Best, J. P.; Zhang, X.; Caruso, F. Super-Soft Hydrogel Particles with Tunable Elasticity in a Microfluidic Blood Capillary Model. *Adv. Mater.* **2014**, *26*, 7295-7299.

(28) Cui, J.; Yan, Y.; Wang, Y.; Caruso, F. Templated Assembly of Ph-Labile Polymer-Drug Particles for Intracellular Drug Delivery. *Adv. Funct. Mater.* **2012**, *22*, 4718-4723.

(29) Wang, Y.; Bansal, V.; Zelikin, A. N.; Caruso, F. Templated Synthesis of Single-Component Polymer Capsules and Their Application in Drug Delivery. *Nano Lett.* **2008**, *8*, 1741-1745.

(30) Haffer, S.; Tiemann, M.; Fröba, M. Periodic Mesoporous Organosilica (PMO) Materials with Uniform Spherical Core-Shell Structure. *Chem. Eur. J.* **2010**, *16*, 10447-10452.

(31) Yoon, S. B.; Kim, J.-Y.; Kim, J. H.; Park, Y. J.; Yoon, K. R.; Park, S.-K.; Yu, J.-S. Synthesis of Monodisperse Spherical Silica Particles with Solid Core and Mesoporous Shell: Mesopore Channels Perpendicular to the Surface. *J. Mater. Chem.* **2007**, *17*, 1758-1761.

(32) Zhang, K.; Xu, L. L.; Jiang, J. G.; Calin, N.; Lam, K. F.; Zhang, S. J.; Wu, H. H.; Wu, G. D.; Albela, B.; Bonneviot, L. *et al.* Facile Large-Scale Synthesis of Monodisperse Mesoporous Silica Nanospheres with Tunable Pore Structure. *J. Am. Chem. Soc.* **2013**, *135*, 2427-2430.

(33) Bagatolli, L.; Sunil Kumar, P. B. Phase Behavior of Multicomponent Membranes: Experimental and Computational Techniques. *Soft Matter* **2009**, *5*, 3234-3248.

(34) Lasch, J.; Weissing, V.; Brandl, M., Preparation of Liposomes. In *Liposomes: A Pratical Approach*; Torchilin, V. P., Weissig, V., Eds.; Oxford Universty Press: New York, 2003; pp 3-27.

(35) Richardson, J. J.; Ejima, H.; Lörcher, S. L.; Liang, K.; Senn, P.; Cui, J.; Caruso, F. Preparation of Nano-and Microcapsules by Electrophoretic Polymer Assembly. *Angew. Chem. Int. Ed.* **2013**, *52*, 6455-6458.

(36) Richardson, J. J.; Liang, K.; Kempe, K.; Ejima, H.; Cui, J.; Caruso, F. Immersive Polymer Assembly on Immobilized Particles for Automated Capsule Preparation. *Adv. Mater.* **2013**, *25*, 6874-6878.

(37) Lee, L. M.; Heimark, R. L.; Guzman, R.; Baygents, J. C.; Zohar, Y. Low Melting Point Agarose as a Protection Layer in Photolithographic Patterning of Aligned Binary Proteins. *Lab Chip* **2006**, *6*, 1080-1085.

Table of Contents Graphic